Extended x-ray-absorption and electron-energy-loss fine-structure studies of the local atomic structure of amorphous unhydrogenated and hydrogenated silicon carbide

Alain E. Kaloyeros
Department of Physics, State University of New York at Albany, Albany, New York 12222

Richard B. Rizk and John B. Woodhouse
Department of Physics and Materials Research Laboratory, University of Illinois at Urbana-Champaign, Urbana, Illinois 61801

(Received 6 July 1988)

Extended x-ray-absorption (EXAFS) and electron-energy-loss fine-structure (EXELFS) measurements have been performed on amorphous unhydrogenated silicon carbide, *a*-SiC, and amorphous hydrogenated silicon carbide, *a*-SiC:H. Two hydrogenated samples with hydrogen concentrations corresponding, respectively, to H flows of 4 sccm (20% of argon flow) and 8 sccm (40% of argon flow) during the reactive sputtering process, were analyzed (sccm denotes standard cubic centimeters per minute at STP). It is found that short-range order (SRO), consisting of the same tetrahedrally coordinated units present in cubic crystalline *c*-SiC (zinc-blende structure), where a Si atom is surrounded by nearly four C atoms and vice versa, does exist in all the amorphous samples. This SRO, however, is detected only at a level of the first C and Si coordination shells in *a*-SiC and *a*-SiC:H. The structural disorder of the first Si and C coordination shells in all forms of amorphous SiC is somewhat greater than *c*-SiC, and it decreases appreciably as hydrogen is added. The *a*-SiC sample exhibits large Si and C coordination numbers, almost identical to *c*-SiC, a low atomic density, and virtually the same Si—C bond length as *c*-SiC. These results indicate that a relatively small concentration of large voids exist in a highly disordered *a*-SiC matrix. The *a*-SiC:H samples, on the other hand, exhibit a decrease in the C coordination number relative to *a*-SiC, which is independent of H concentration, low Si and C atomic densities, comparable to *a*-SiC, and virtually the same Si coordination number as *a*-SiC. These EXAFS-EXELFS results are consistent with a model where part of the H is substituting for Si in the local tetrahedra surrounding C atoms, while the rest is located inside internal voids in the *a*-SiC:H samples. The surface of the voids is composed of C atoms which have at least one bond to H, and of Si atoms. Finally, a straightforward computational procedure is applied to estimate the size of these voids. It is found that their average size ≥ 21 Å, thus excluding the possibility that the voids might be point defects.

I. INTRODUCTION

In recent years, both amorphous unhydrogenated and hydrogenated silicon carbide (*a*-SiC and *a*-SiC:H) have witnessed considerable increase in research interest attributed primarily to their attractive electronic, optical, and optoelectronic properties, and, consequently, to their potential technological applications.[1–6] Amorphous hydrogenated silicon carbide, for instance, has been proposed as a wide-band-gap intrinsic layer in multilayer amorphous silicon solar cells,[7] and has already been used as a *p*-type window layer in *a*-Si:H solar cells.[8] In addition, because of its high-temperature stability, semiconducting silicon carbide is presently a candidate material in the search for a stable high-temperature semiconductor.[9] It has also been suggested that, since stoichiometry greatly affects the physical properties of *a*-SiC:H (i.e., Si_xC_{1-x}:H), one could exploit the variability of composition x and the concentration of hydrogen incorporated to tailor the electronic properties of the compound to different applications, possibly surpassing amorphous hydrogenated silicon.[10]

However, the behavior of *a*-SiC and *a*-SiC:H is quite complex and, unfortunately, most of their properties do not vary linearly with alloy composition.[11] Many structural studies were thus performed to establish an understanding of the relationship between variations in the composition of these materials and their physical properties.[10,12–14] Although these investigations were widely diverse in scope and content, they all agreed that a knowledge of the structure of these materials at the nanoscopic level—local atomic environment or short-range order (SRO)—is essential to establish a complete understanding of their properties. Nevertheless, many important structural issues remain unresolved, and little is known about the physical mechanisms that govern the inclusion of C and H in the silicon matrix, their local atomic structure, and where the H binds in modifying the amorphous matrix.[15]

Extended x-ray-absorption fine-structure spectroscopy (EXAFS) and extended electron-energy-loss fine-structure spectroscopy (EXELFS) are powerful techniques for probing the nanostructure of amorphous semiconductors.[16] Unfortunately, all researchers using

EXAFS have focused so far on the silicon nanostructure,[12,17–19] while EXELFS has been applied to study the local structure in amorphous carbon,[20] graphitic carbon,[21] and graphite,[22] but not in silicon carbide alloys. The present paper reports on the first application of EXAFS-EXELFS to study the local atomic environment of both Si and C atoms in stoichiometric *a*-SiC and *a*-SiC:H. Information generated on the SRO and the nanostructural static disorder σ^2 about the silicon and carbon atoms and on the location of H and its effects on the amorphous silicon carbide matrix is presented and discussed. In what follows, we summarize the details of the measurements and of sample preparation in Sec. II. The EXAFS-EXELFS formalism and data analysis are explained in Sec. III, while a discussion and an interpretation of the results are given in Sec. IV. Finally, the main conclusions are outlined in Sec. V.

II. EXPERIMENT

a-SiC and *a*-SiC:H thin films were prepared on quartz substrates by conventional radio-frequency (rf) reactive sputtering (13.56 MHz) in an argon atmosphere (*a*-SiC) and in an argon-hydrogen mixture (*a*-SiC:H). The surface of the substrates was mechanically roughened to suppress any optical interference effects. High-resistivity composite targets of high-purity (99.999%) silicon base plate and carbon chips were employed and the carbon-to-silicon area ratio in the target changed until stoichiometry was achieved in the sputtered films. All sets of samples, hydrogenated or not, were deposited under the same experimental conditions, except for hydrogen flow. The base pressure of the sputtering apparatus was less than 1×10^{-7} torr, and the argon partial pressure was held constant, for all deposition runs at $P_{\mathrm{Ar}}\sim5\times10^{-3}$ torr (Ar flow of 20 sccm, where sccm denotes cubic centimeters per minute at STP). Upon hydrogenation, the hydrogen partial pressure was set at, for different deposition runs, $P_{\mathrm{H_2}}\sim0.6$ and 1.2×10^{-3} torr, corresponding to hydrogen flows of 4 sccm (20% of Ar flow) and 8 sccm (40% of Ar flow), respectively, thus allowing us to produce films with variable hydrogen concentrations. The rf input power of 100 W was applied to the sputtering target of 15 cm^2 surface area, which corresponded to a power density of ~6.66 $\mathrm{W/cm}^2$. The deposition rate was nearly constant at ~5 Å/s for hydrogen partial pressures below 0.6×10^{-3} torr, but gradually decreased to ~3 Å/s at the hydrogen partial pressure of 1.2×10^{-3} torr. The films were produced with thicknesses below 200 Å.

The EXAFS-EXELFS studies were carried out at the Center for Microanalysis of Materials, Materials Research Laboratory, University of Illinois at Urbana-Champaign.

The experimental measurements employing a high-energy electron beam (300 keV) were performed on a Philips EM430 transmission electron microscope (TEM) equipped with a Gatan model 607 single magnetic sector, double-focusing electron-energy-loss spectrometer. The electron microscope was used in the bright-field imaging mode to form a 1-μm-diam probe on the specimen with a beam current of ~1 μA. An entrance slit to the spectrometer selected electrons according to their scattering angle and the spectrometer dispersed them in a direction perpendicular to the slit. Spectra were recorded by scanning the energy-loss intensity across an apertured scintillator (model NE100) and by counting the single pulses derived from the photomultiplier (RCA 8575). An EDAX 9100/60 multichannel analyzer-minicomputer, equipped with acquisition and display facilities, was used for data gathering and initial processing. Thermal vibration effects[23] were minimized by mounting the TEM samples in a Philips model PW6591/01 side-entry cold stage and performing measurements with liquid-nitrogen cooling at 80 K.

Since the extended fine structure above the core edges consists of small intensity modulations ranging in amplitude typically from 10% near the ionization threshold to less than 1%, a few hundred eV higher in energy, statistics are required to be at the 1%—possibly 0.1%—signal-to-noise level.[24] This corresponds in silicon carbide spectra to between 10^5 and 10^6 counts per channel for the typical background intensities preceding the edges, which required a check of the reliability of the counting rates achievable with our system. Following the procedure of Leapman, Rez, and Mayers,[25] we found that minimum counting times of ~2 s per eV channel are needed at the silicon and carbon core edges. However, because of the decreasing cross section above threshold, the average time per channel used was 3 s.[26]

Multiple-scattering effects, such as collective plasmons, were also minimized by limiting the sample thickness to $\sim1.5\lambda$ (where λ is the inelastic mean free path), leading to typical thicknesses below 200 Å. The plural-scattering processes tend to induce distortions and inaccuracies in the analysis, such as extra peaks in the spectrum above the edge and an increase in the background intensity relative to the signal, and it is of major importance that they are accounted for. The *a*-SiC:H films, of thicknesses below 200 Å, were removed from the substrates by etching with hydrofluoric acid and collected on copper microscope grids to make samples of optimum thickness. Crystalline silicon carbide (*c*-SiC) samples, used as standards, were prepared as thin, 3-mm-diam disks by using an annular diamond saw and an ultrasonic drill. The disks were subsequently polished on a series of laps and cloths and finally thinned to perforation using an ion-beam milling machine.

III. EXAFS-EXELFS FORMALISM AND DATA ANALYSIS

The general theory and interpretation of EXAFS-EXELFS are now well established and will not be discussed in detail in the present paper.[27–29] A brief outline of the important steps of the EXAFS-EXELFS data analysis will be presented, however, to aid in the understanding of the data processing and of the results presented.

The equation of EXAFS-EXELFS modulations $\chi(k)$, assuming no multiple scattering, is given by[30]

$$\chi(k)=\sum_j \frac{N_j A_j}{kR_j^2} e^{-2k^2\sigma_j^2} e^{-2R_j/\lambda} \sin(2kR_j+\lambda_j) .$$

The summation is over coordination shells of atoms surrounding the excited atom, with N_j (the coordination number) atoms in shell j located at an average distance R_j from the central atom. The first exponential term accounts for the motion of the atoms due to thermal (as well as zero-point) vibrations and to static displacements. The parameter σ_j^2 is the mean-square relative displacement for the jth shell, and the electron wave vector k is related to the emitted electron's energy E by $k=(2m_e E/\hbar^2)^{1/2}$. The quantity λ is the phenomenological mean free path that corresponds to a finite lifetime of the excited state, $A_j(2k)$ is the backscattering amplitude of the atoms in the jth shell, and $\delta_j(k)$ is the phase shift experienced by the photoelectron as it traverses the potential of the central and backscattering atoms.

Experimentally, the EXAFS-EXELFS spectra appear as low-intensity oscillations (relative to the jump at the ionization edge) superimposed on the smooth atomic background, which decays with increasing energy above the edge. These oscillations are observed in the "raw" data that we collected; for instance, for EXELFS above the Si L edges at 99.2 eV ($L_{2,3}$ edges) and at 149 eV (L_1 edge), the C K edge at 283.9 eV, and the Si K edge at 1839 eV in a-SiC:H [see Figs. 1(a) and 1(b)]. The data have not been smoothed or normalized, nor has any background been removed.

First, it is necessary to isolate the elemental oscillatory modulations $\chi(k)$ from the smooth atomic background by fitting and removing the preedge background due to other edges and to the other elements. The edge step is then normalized so that comparisons could be made between spectra from different samples. The normalized spectrum is transformed to k space using the relation $\hbar^2k^2/2m=E-E_0$, where E_0 is the excitation energy. E_0 is taken as the energy about the first inflection point at the threshold for ionization.[30] $\chi(k)$ is consequently isolated by means of a cubic spline fit and background subtraction. We performed this procedure to isolate the $\chi(k)$ data for the Si and C K edges in all four types of samples [crystalline SiC, a-SiC, a-SiC:H (20% H_2 flow), and a-SiC:H (40% H_2 flow)].

From $\chi(k)$, a radial distribution function, or RDF, $F(R)$ can be derived by Fourier transforming $\chi(k)$ to R space. The resulting $F(R)$ gives a rough idea of the coordination numbers and locations of the surrounding atoms and is only an intermediate step. The positions of the peaks in $F(R)$ are shifted compared to the true distances as a result of excluding from the Fourier transform the contribution from the phase shifts $\delta_j(k)$, which are k dependent. Figures 2 and 3 show the radial distribution functions for the Si and C atoms in, respectively, cubic crystalline SiC and a-SiC:H (20% H_2 flow).

Next, a shell is selected using a smooth window and back-Fourier-transforming to k space is carried out to isolate the single-shell contribution to the $\chi(k)$ data. The final stage of the analysis involves determining structural parameters (coordination number, radial distance, and structural disorder σ^2) for the unknowns, namely, a-SiC and a-SiC:H. For this purpose, the ratio method is applied.[16,27,28] It involves comparing the single-shell data from the unknown with those from a suitable standard of known structure and a chemical environment which is similar to the unknown structure. Clearly, crystalline SiC can be used as the standard in this case. The chemical transferability of the phase shifts and backscattering amplitudes is well established, since the local environment and chemical state (local bonding) should not differ considerably between the crystalline and amorphous states. The use of the ratio method thus reduces reliance on the assumption of transferability and allows high accuracy to be achieved in the determination of structural parameters. In Fig. 4, we display a representative phase difference and logarithmic amplitude ratio of a-SiC as compared to c-SiC. The error bars in the curves reflect the difference in results obtained from an independent analysis of different scans and is a measure of the noise in the data and any systematic noise introduced in the analysis.[31,32]

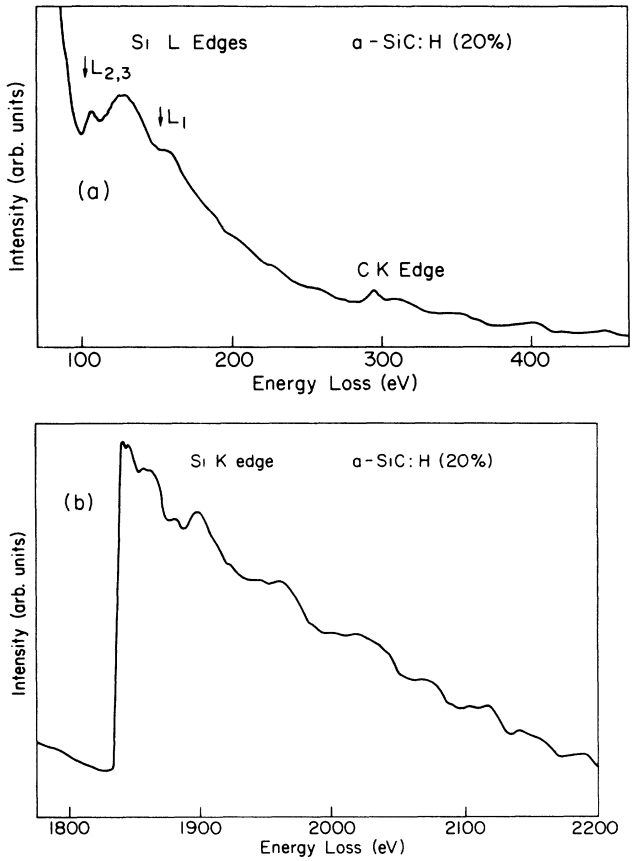

FIG. 1. Typical "raw" electron-energy-loss data, showing extended fine structure, past (a) the Si L edges and the C K edge, and (b) the Si K edge in a-SiC:H (20% H_2 flow). The data have not been normalized, smoothed, or edited.

IV. RESULTS AND DISCUSSION

As can be seen from Figs. 2 and 3, the transform, or radial distribution function $F(R)$, contains only a first-shell

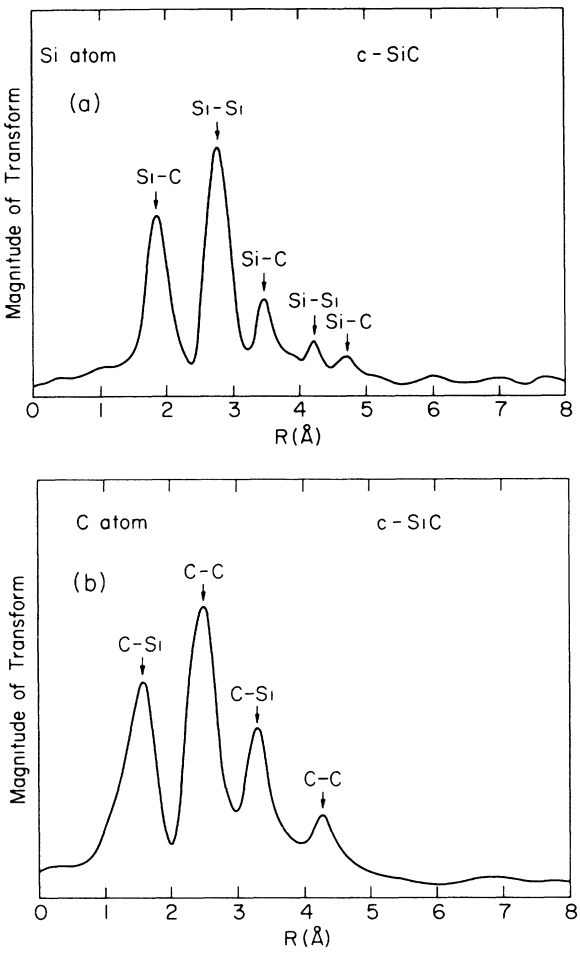

FIG. 2. Magnitudes of Fourier transforms of $\chi(k)$ measured at the K edges for (a) a Si atom, and (b) a C atom in cubic c-SiC.

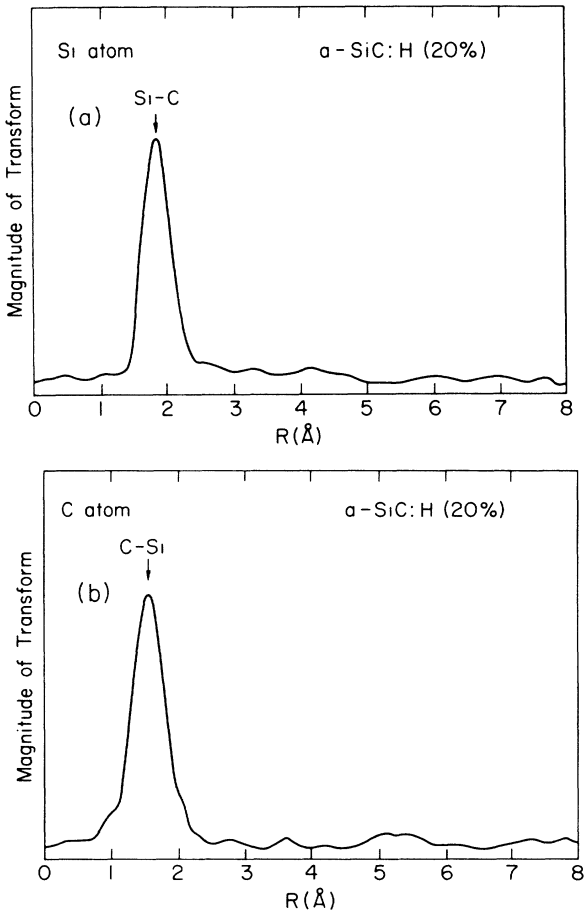

FIG. 3. Magnitudes of Fourier transforms of $\chi(k)$ measured at the K edges for (a) a Si atom, and (b) a C atom in a-SiC:H (20% H_2 flow).

signal for a-SiC:H (20% H_2 flow), while that corresponding to cubic crystalline SiC (c-SiC) shows clear contributions from at least five separate coordination shells for Si and four distinct coordination shells for C. Similarly, only first-shell signals were detected for a-SiC and a-SiC:H (40% H_2 flow). The EXAFS-EXELFS results clearly indicate that the amorphous phases, whether hydrogenated or not, are not formed of random arrangements of Si and C atoms, but exhibit short-range order at the level of the first coordination shell only.[33,34]

The existence of SRO at the level of the first-nearest-neighbor shell only in the silicon carbide amorphous phases (a-SiC and a-SiC:H) greatly simplifies the use of crystalline SiC as standard in applying the ratio method. Crystalline SiC exhibits an exceptionally wide range of polytypes in its crystalline structure.[35] Silicon carbide crystals not only occur in cubic and hexagonal zinc blende (zinc sulfide) structures, but also in 45 other known stacking sequences of the hexagonal layers.[36,37] However, all nearest-neighbor bonds are tetrahedral in both schemes and in the variations of the hexagonal structure. If we look only at the nearest-neighbor atoms to a given atom, we cannot tell whether we are in a cubic or hexagonal crystal, but if we look beyond the nearest-neighbor atoms to the second-nearest-neighbor atoms we can distinguish the cubic and hexagonal forms. Furthermore, the nearest-neighbor bond lengths are quite close in the two structure—1.883 Å in cubic SiC, 1.990 Å in hexagonal SiC. Since we are comparing only first coordination shell signal in the unknowns (a-SiC, a-SiC:H) to that from the standard (c-SiC), either c-SiC form could be used. However, practical considerations and the expectation that the most stable amorphous SiC form involves the cubic modification[10] motivated our choice of cubic c-SiC as the standard.

In Tables I and II, we report structural parameters (interatomic distances, coordination numbers, and structural disorder $\Delta\sigma^2$) for all three amorphous samples, deduced by the ratio method. A relatively high precision in the determination of structural information is achieved through the use of an absolute calibration procedure presented initially by Bouldin, Stern, von Roedern, and Azoulay.[15,38] The most important observation is perhaps that the SRO observed in all amorphous films—both hydrogenated and unhydrogenated—consists basically of the same tetrahedrally coordinated units observed in cu-

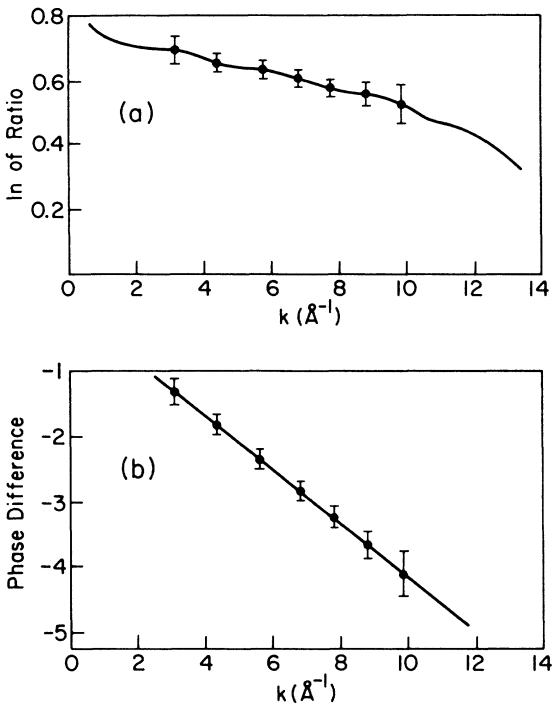

FIG. 4. (a) Logarithm of amplitude ratio between a-SiC and c-SiC; (b) the corresponding phase difference. Both samples were measured at 80 K and their relative E_0 has been adjusted by 0.4 eV so that the phase inercept at $k=0$ passes through a multiple of $2n\pi$.

bic c-SiC, where a silicon atom is surrounded approximately by four C atoms and vice versa, as seen in column 2 of both tables.

In the first column of Tables I and II, we report the density ρ of Si and C atoms in the amorphous films, as deduced from the magnitude of the jump of the Si and CK ionization edges relative to the density ρ of their counterparts in c-SiC. The a-SiC sample exhibits a high reduction of ρ with respect to ρ_c and a large increase in structural disorder about both Si and C atoms in comparison to c-SiC (see the corresponding $\Delta\sigma^2$ values in column 4), but virtually no change in the Si—C bond length.

The corresponding coordination numbers N, as deduced from the EXAFS-EXELFS analysis, of Si and C are reported in column 2. We note that the a-SiC sample exhibits a large coordination, almost identical to that of c-SiC, despite its low atomic density. These observations point to the possible presence of a relatively small concentration of large voids in a highly disordered a-SiC structure. Only voids can explain the results of decreased density because of the comparably insignificant changes in coordination number and nearest-neighbor distance in a-SiC.

Next, we attempt to understand how the hydrogen binds in modifying the amorphous structure. The addition of hydrogen, within the experimental error of $\sim 5\%$, causes a decrease in the coordination number of carbon in the hydrogenated samples of $\sim 6.25\%$ relative to c-SiC, and this is the same for both a-SiC:H (20% H_2 flow) and a-SiC:H (40% H_2 flow). The comparison with a-SiC indicates a coordination number decrease of $\sim 6\%$ which is independent of hydrogen concentration. No change is detected, to within the experimental error, for the coordination number of silicon in the hydrogenated samples relative to c-SiC. Similarly, the Si—C bond length remains virtually unchanged.

Within the cited errors, these results are consistent and indicate that in the hydrogenated samples, hydrogen bonds mainly to carbon. Since the H atoms are invisible to EXAFS because of their low backscattering amplitude at $k > 3$ Å^{-1}, their binding to C would cause a decrease in coordination number as measured by EXAFS-EXELFS.[15,39]

One hypothesis is that a hydrogen atom binds to one C atom without displacing any C—Si bonds. If this occurred, then some of the C atoms would have five bonds consisting of four Si neighbors and a fifth bond due to hydrogen. This hypothesis is implausible from chemical arguments since C atoms tend to form four covalent bonds.[38] Furthermore, the addition of a fifth bond would be expected to change the distances of the four C-Si nearest neighbors and would tend to also increase $\Delta\sigma^2$, the opposite of what is observed experimentally. Finally, this possibility is precluded on the basis that it does not account for the reduction in the C coordination number with hydrogen addition.

A second possibility is that H substitutes for Si in the locally ordered tetrahedral unit, made predominantly of Si atoms, surrounding a C atom. This hypothesis is supported by the experimental observation that the coordination number of carbon exhibits a decrease with hydrogen addition, while the coordination number of Si, i.e., the number of C atoms in the locally ordered tetrahedral units surrounding Si atoms, does not change.

The decrease in carbon nearest-neighbor coordination is not, however, the only significant structural change observed upon hydrogenation. A decrease in σ^2 of the Si and C atoms, which is proportional to hydrogen addition, is also observed. The presence of hydrogen during the sputtering process may tend to increase the surface mo-

TABLE I. Interatomic distances, coordination numbers, and structural disorder for the Si atom in c-SiC, a-SiC, a-SiC:H (20% H_2 flow), and a-SiC:H (40% H_2 flow).

Sample	ρ/ρ_c	N	R (Å)	$\Delta\sigma^2$ (10^{-3} Å^2)
c-SiC	1.00	4.00	1.88 (3)	0.0
a-SiC	0.86 (3)	3.99 (5)	1.86 (3)	3.5 (6)
a-SiC:H (20% H_2 flow)	0.85 (2)	3.98 (4)	1.87 (2)	2.2 (5)
a-SiC:H (40% H_2 flow)	0.84 (3)	3.98 (4)	1.89 (2)	1.5 (6)

TABLE II. Interatomic distances, coordination numbers, and structural disorder for the C atom in *c*-SiC, *a*-SiC, *a*-SiC:H (20% H_2 flow), and *a*-SiC:H (40% H_2 flow).

Sample	ρ/ρ_c	N	R (Å)	$\Delta\sigma^2$ (10^{-3} Å^2)
c-SiC	1.00	4.00	1.88 (3)	0.0
a-SiC	0.83 (3)	3.98 (4)	1.86 (3)	4.1 (7)
a-SiC:H (20% H_2 flow)	0.85 (2)	3.75 (5)	1.87 (2)	2.5 (5)
a-SiC:H (40% H_2 flow)	0.84 (2)	3.74 (4)	1.89 (2)	1.8 (5)

bility of the Si and C atoms in such a way as to produce a locally more ordered material even though the incorporation of H inhibits crystallization, i.e., the crystallization temperature for the hydrogenated samples is found to be a few hundred degrees higher than for *a*-SiC.[15,16,38,40] This decrease in σ^2 for *both* the silicon and carbon atoms upon hydrogenation, and the fact that the decrease in C coordination number is independent of the amount of hydrogen incorporated, seems to indicate that H substitution for Si is not the only mechanism involved in the hydrogenation of amorphous silicon carbide.

The only remaining possibility is that hydrogen is located inside internal voids in amorphous silicon carbide. The surface of the voids is composed of carbon atoms which have at least one bond to a hydrogen atom, and of silicon atoms. This model explains the experimental results of decreased density and reduced coordination number for C which is independent of H concentration.

As pointed out by Bouldin *et al.*,[15] voids will both decrease the density proportional to their volume and decrease the coordination number proportional to their surface area. We can combine the EXAFS-EXELFS density and coordination-number measurements to estimate the size of these voids. We follow the procedure of Bouldin *et al.*[38] which assumes that (1) C surface atoms bond one H atom, (2) voids are cubic in shape, and (3) except for the voids, the densities of the amorphous and crystalline phases are the same, consistent with the experimental observations of invariant nearest-neighbor distance and nearest-neighbor coordination number. In other words, the bulk densities of the two phases between voids are essentially equal. The results of the analysis are not expected to change significantly if the voids were of some other compact shape, e.g., spherical.

We consider cubic *c*-SiC which has the zinc-blende structure with eight atoms (four Si and four C) per cubic unit cell of side a. The volume per atom is thus $(a/2)^3$ which leads to an atomic density $A^3/(a/2)^3=8A^3/a^3$ per cubic of side A. The surface area per atom is $(a/2)^2$ which gives an atomic surface density, for a cube of surface area $6A^2$, of $6A^2/(a/2)^2=24A^2/a^2$. Consequently, the ratio of total number of atoms n_v to that of surface atoms n_s in a cube of side A is

$$\frac{n_v}{n_s}=\frac{1}{3}\frac{A}{a} . \tag{1}$$

Next, we examine the effects of taking out a cubic void of side A consisting of n_v atoms and n_s surface atoms. The n_v atoms would decrease the density by $\Delta\rho/\rho=n_v(a/2)^3$, while the n_s surface atoms would reduce the coordination per atom by $\Delta N/N=\frac{1}{4}n_s(a/2)^3$. The corresponding ratio is thus

$$\left[\frac{\Delta\rho}{\rho}\Big/\frac{\Delta N}{N}\right]=\frac{4n_v}{n_s} . \tag{2}$$

Combining with (1), we find, for a cubic void of side A,

$$A=\frac{3a}{4}\frac{\Delta\rho}{\rho}\frac{\Delta N}{N} . \tag{3}$$

From the EXAFS-EXELFS results, we find that at $T\sim 80$ K the average change in atomic density with respect to *c*-SiC, computed from the magnitude of the jumps of the Si and C K edges in all three amorphous samples, is $\Delta\rho/\rho\sim 0.155\pm 0.02$. Averaging $\Delta N/N$ for the Si and C atoms of the three amorphous samples compared to the crystalline sample, we obtain $\Delta N/N\sim 0.024\pm 0.005$. Substituting these values into Eq. (3) and using the lattice constant of cubic *c*-SiC of 4.35 Å we obtain $A\geq 21$ Å. This void-size estimate applies to both *a*-SiC and *a*-SiC:H on the basis that their atomic densities are practically the same. More importantly, this result seems to indicate that the voids have dimensions significantly larger than atomic sizes and, consequently, could not be point defects. Previous work concluded that point defects have typical sizes of ≤ 7 Å,[41] and although our estimates are not highly accurate, voids less than 7 Å in size are clearly excluded by our EXAFS-EXELFS measurements.

In summary, our EXAFS-EXELFS results are consistent with a structural model where at least part of the hydrogen is saturating carbon bonds on the surfaces of large voids in amorphous silicon carbide, while the rest of the hydrogen is substituting for silicon atoms in the locally ordered tetrahedra surrounding C atoms.

V. CONCLUSIONS AND SUMMARY

Within the cited errors, we conclude the following.

1. The SRO observed in the unhydrogenated and hydrogenated amorphous silicon carbide samples consists of basically the same tetrahedrally coordinated units observed in cubic *c*-SiC, where a C atom is surrounded by nearly four Si atoms and vice versa. However, these ordered units are observed at the level of the first coordination shell in *a*-SiC, *a*-SiC:H (20% H_2 flow), and *a*-SiC:H (40% H_2 flow).

2. The *a*-SiC sample exhibits a large coordination number for both the Si and C atoms, almost identical to

that of *c*-SiC, a low atomic density, virtually the same Si—C bond length as *c*-SiC, and a large increase in structural disorder about the Si and C atoms in comparison to *c*-SiC. These observations point to the possible presence of a relatively small concentration of large voids in a highly disordered *a*-SiC matrix.

3. Upon hydrogenation, a decrease in the C coordination number, which is independent of the amount of H incorporated, is observed for *a*-SiC:H (20% H_2 flow) and *a*-SiC:H (40% H_2 flow) with respect to *a*-SiC. A reduction in the carbon structural disorder, which is, however, proportional to hydrogen concentration, is also detected relative to *a*-SiC. These changes indicate that a partial H substitution for Si is occurring in the locally ordered tetrahedral units, made predominantly of Si atoms, surrounding C atoms. No such decrease is observed in the Si coordination number with hydrogen doping.

4. Other structural effects are also detected upon hydrogenation, primarily a simultaneous decrease in the structural disorder about the Si and C atoms in *a*-SiC:H (20% H_2 flow), *a*-SiC:H (40% H_2 flow) relative to *a*-SiC, and a low Si and C atomic density comparable to *a*-SiC. The decrease is proportional to the amount of H incorporated. These additional changes, and the fact that the reduction in C coordination number is independent of H concentration, seem to indicate that the mechanism proposed in conclusion 3 is not the only one involved in the hydrogenation of amorphous silicon carbide. We propose an additional model where H atoms are located inside internal voids in amorphous SiC. The surface of the voids is composed of carbon atoms which have at least one bond to a hydrogen atom, and of silicon atoms. This model explains the experimental results of decreased density, reduced structural disorder about Si and C, and reduced coordination number for C which is independent of H concentration. Our EXAFS-EXELFS results are consistent and seem to indicate that part of the H is bound to the C surface atoms while the rest substitute for Si in the local tetrahedra surrounding C atoms.

5. A computational procedure, initially proposed by Bouldin *et al.*,[15] is applied to estimate the size of these internal voids. It is found that the average void size is ≥ 21 Å for both *a*-SiC and *a*-SiC:H on the basis that their atomic densities are practically the same. Our EXAFS-EXELFS measurements indicate that the voids are significantly larger than atomic sizes, and thus are not point defects.

ACKNOWLEDGMENTS

This work was supported by the National Science Foundation under Grant No. MSM 8617318, which is gratefully acknowledged. The analyses were carried out at the Center for Microanalysis of Materials of the University of Illinois at Urbana-Champaign Materials Research Laboratory (MRL), which is supported by the U.S. Department of Energy under contract No. DE-AC02-76ER01198. We thank professional staff members Nancy Finnegan, Joyce McMillan, and Alex Greene for their help and advice. Special thanks to Professor Wendell S. Williams for his extremely helpful suggestions, his enlightening discussions, and for allowing access to his laboratories and use of his experimental apparatus. One author (R.B.K.) would like to acknowledge the United States Information Agency (USIA)–Fulbright Program, which made his contributions to this work possible.

[1]M. A. Petrich, K. K. Gleason, and J. A Reimer, Phys. Rev. B **36**, 9722 (1987).

[2]R. Biswas, G. S. Grest, and C. M. Soukoulis, Phys. Rev. B **36**, 7437 (1987).

[3]A. Bianconi, A. DiCicco, N. V. Pavel, M. Benfatto, A. Marcelli, C. R. Natoli, P. Pianetta, and J. Woicik, Phys. Rev. B **36**, 6426 (1987).

[4]P. J. H. Denteneer and W. van Haeringen, Solid State Commun. **59**, 829 (1986).

[5]N. Churcher, K. Kunc, and V. Heine, Solid State Commun. **56**, 177 (1985).

[6]S. H. Sie, C. G. Ryan, D. R. McKenzie, and G. B. Smith, Nucl. Instrum. Methods Phys. Res. B **15**, 632 (1986).

[7]R. Könenkamp, Phys. Rev. B **36**, 2938 (1987).

[8]F. Fujimoto, A. Ootuka, K. Komaki, Y. Iwata, I. Yamane, H. Yamashita, Y. Hashimoto, Y. Tawada, K. Nishimura, H. Okamoto, and Y. Hamakawa, Jpn. J. Appl. Phys. **23**, 810 (1984).

[9]Y. Li and P. J. Lin-Chung, Phys. Rev. B **36**, 1130 (1987).

[10]P. Morgen, K. L. Seaward, and T. W. Barbee, Jr., J. Vac. Sci. Technol. A **3**, 2108 (1985).

[11]D. A. Anderson and W. E. Spear, Philos. Mag. B **35**, 1 (1977).

[12]C. Laffon, A. M. Flank, and P. Lagarde, J. Phys. (Paris) Colloq. **47**, C8-383 (1986).

[13]G. H. Bauer, H. D. Mohring, G. Bilger, and A. Eicke, J. Non-Cryst. Solids **77-78**, 873 (1985).

[14]J. C. Anderson, S. Biswas, and H. Guo, J. Appl. Phys. **61**, 604 (1987).

[15]C. E. Bouldin, E. A. Stern, B. von Roedern, and J. Azoulay, Phys. Rev. B **30**, 4462 (1984).

[16]A. E. Kaloyeros, W. S. Williams, F. C. Brown, A. E. Greene, and J. B. Woodhouse, Phys. Rev. B **37**, 771 (1988).

[17]D. E. Sayers and M. A. Paesler, J. Phys. (Paris) Colloq. **47**, C8-349 (1986).

[18]A. J. Bourdillon, N. W. Jepps, W. M. Stobbs, and O. L. Krivanek, J. Microsc. **124**, 49 (1981).

[19]A. Menelle, A. M. Flank, P. Lagarde, and R. Bellissent, J. Phys. (Paris) Colloq. **47**, C8-379 (1986).

[20]J. Fink, T. Müller-Heinzerling, J. Pflüger, A. Rubenzer, P. Koidl, and G. Crecelius, Solid State Commun. **47**, 687 (1983).

[21]S. Modesti, M. De Crescenzi, P. Perfetti, C. Quaresima, R. Rosei, A. Savoia, and F. Sette, in *EXAFS and Near-Edge Structure,* edited by A. Bianconi, L. Incoccia, and S. Stipcich (Springer-Verlag, Berlin, 1983), p. 394.

[22]S. Csillag, D. E. Johnson, and E. A. Stern, in *EXAFS Spectroscopy; Techniques and Applications,* edited by B. K. Teo and D. C. Joy (Plenum, New York, 1981), p. 241.

[23]J. M. Tranguada, S. M. Heald, and A. R. Moodenbaugh, Phys. Rev. B **36**, 8501 (1987).

[24]R. D. Leapman, L. A. Grunes, P. L. Fejes, and J. Silcox, in *EXAFS Spectroscopy; Techniques and Applications,* edited by B. K. Teo and D. C. Joy (Plenum, New York, 1981), p. 217.

[25]R. D. Leapman, P. Rez, and D. F. Mayers, J. Chem. Phys. **72**, 1232 (1980).

[26]A. E. Kaloyeros, W. S. Williams, R. B. Rizk, F. C. Brown, and A. E. Greene, J. Am. Ceram. Soc. (to be published).
[27]E. A. Stern and S. M. Heald, in *Handbook on Synchrotron Radiation,* edited by E. E. Koch (North-Holland, Amsterdam, 1983), Vol. 1, p. 955.
[28]B. K. Teo, *EXAFS: Basic Principles and Data Analysis* (Springer-Verlag, Berlin, 1986), p. 21.
[29]A. E. Kaloyeros, M. P. Hoffman, W. S. Williams, A. E. Greene, and J. A. McMillan, Phys. Rev. B (to be published).
[30]E. A. Stern and J. J. Rehr, Phys. Rev. B **27**, 3351 (1983).
[31]G. Stegemann and B. Lengeler, J. Phys. (Paris) Colloq. **47**, C8-407 (1986).
[32]B. Lengeler, Z. Phys. B **61**, 421 (1985).
[33]A. Filipponi, P. Fiorini, F. Evangelisti, A. Balerna, and S. Mobilio, J. Phys. (Paris) Colloq. **47**, C8-357 (1986).
[34]A. Filipponi, D. Della Sala, F. Evangelisti, A. Balerna, and S. Mobilio, J. Phys. (Paris) Colloq. **47**, C8-375 (1986).
[35]D. E. Carlson, J. Vac. Sci. Technol. **20**, 290 (1982).
[36]A. R. Verma and P. Krishna, *Polymorphism and Polytypism in Crystals* (Wiley, New York, 1966).
[37]A. R. Verma, in *Silicon Carbide,* edited by J. R. O'Connor and J. Smiltens (Pergamon, New York, 1960), Chap. 20.
[38]C. E. Bouldin, E. A. Stern, B. von Roedern, and J. Azoulay, J. Non-Cryst. Solids **66**, 105 (1984).
[39]P. H. Citrin, P. Eisenberger, and B. M. Kincaid, Phys. Rev. Lett. **36**, 1346 (1976).
[40]A. E. Kaloyeros, C. M. Allocca, W. S. Williams, D. M. Pollina, and G. S. Girolami, Adv. Ceram. Mater. **2**, 100 (1987).
[41]G. A. N. Connell and J. R. Pawlik, Phys. Rev. B **13**, 787 (1976); R. J. Temkin, W. Paul, and G. A. N. Connell, Adv. Phys. **22**, 581 (1973).